1-1-2012

Trapping and rotating microparticles and bacteria with moire-based optical propelling beams

Peng Zhang

Daniel Hernandez

Drake Cannan

Yi Hu

Shima Fardad
University of Central Florida

See next page for additional authors

Folate receptor targeting silica nanoparticle probe for two-photon fluorescence bioimaging

Xuhua Wang,[1] Sheng Yao,[1] Hyo-Yang Ahn,[1] Yuanwei Zhang,[1] Mykhailo V. Bondar,[1,3] Joseph A. Torres,[1,4] and Kevin D. Belfield[1,2,*]

[1] *Department of Chemistry, University of Central Florida, FL, Orlando, 32816, USA*
[2] *CREOL, The College of Optics and Photonics, University of Central Florida, FL, Orlando, 32816, USA*
[3] *Institute of Physics, Prospect Nauki, 46, Kiev-28, 03028, Ukraine*
[4] *Department of Chemistry, New Mexico Highland University, NM, Las Vegas, 87701, USA*
belfield@mail.ucf.edu

Abstract: Narrow dispersity organically modified silica nanoparticles (SiNPs), diameter ~30 nm, entrapping a hydrophobic two-photon absorbing fluorenyl dye, were synthesized by hydrolysis of triethoxyvinylsilane and (3-aminopropyl)triethoxysilane in the nonpolar core of Aerosol-OT micelles. The surface of the SiNPs were functionalized with folic acid, to specifically deliver the probe to folate receptor (FR) over-expressing Hela cells, making these folate two-photon dye-doped SiNPs potential candidates as probes for two-photon fluorescence microscopy (2PFM) bioimaging. *In vitro* studies using FR over-expressing Hela cells and low FR expressing MG63 cells demonstrated specific cellular uptake of the functionalized nanoparticles. One-photon fluorescence microscopy (1PFM) imaging, 2PFM imaging, and two-photon fluorescence lifetime microscopy (2P-FLIM) imaging of Hela cells incubated with folate-modified two-photon dye-doped SiNPs were demonstrated.

OCIS codes: (170.0170) Medical optics and biotechnology; (170.3880) Medical and biological imaging; (170.2520) Fluorescence microscopy.

References and links

1. W. Denk, J. H. Strickler, and W. W. Webb, "Two-photon laser scanning fluorescence microscopy," Science **248**(4951), 73–76 (1990).
2. R. M. Williams, W. R. Zipfel, and W. W. Webb, "Multiphoton microscopy in biological research," Curr. Opin. Chem. Biol. **5**(5), 603–608 (2001).
3. V. E. Centonze, and J. G. White, "Multiphoton excitation provides optical sections from deeper within scattering specimens than confocal imaging," Biophys. J. **75**(4), 2015–2024 (1998).
4. J. M. Squirrell, D. L. Wokosin, J. G. White, and B. D. Bavister, "Long-term two-photon fluorescence imaging of mammalian embryos without compromising viability," Nat. Biotechnol. **17**(8), 763–767 (1999).
5. A. R. Morales, K. J. Schafer-Hales, A. I. Marcus, and K. D. Belfield, "Amine-reactive fluorene probes: synthesis, optical characterization, bioconjugation, and two-photon fluorescence imaging," Bioconjug. Chem. **19**(12), 2559–2567 (2008).
6. C. D. Andrade, C. O. Yanez, L. Rodriguez, and K. D. Belfield, "A series of fluorene-based two-photon absorbing molecules: synthesis, linear and nonlinear characterization, and bioimaging," J. Org. Chem. **75**(12), 3975–3982 (2010).
7. A. R. Morales, C. O. Yanez, K. J. Schafer-Hales, A. I. Marcus, and K. D. Belfield, "Biomolecule labeling and imaging with a new fluorenyl Two-photon fluorescent probe," Bioconjug. Chem. **20**(10), 1992–2000 (2009).
8. M. Ferrari, "Cancer nanotechnology: opportunities and challenges," Nat. Rev. Cancer **5**(3), 161–171 (2005).
9. E. Ruoslahti, S. N. Bhatia, and M. J. Sailor, "Targeting of drugs and nanoparticles to tumors," J. Cell Biol. **188**(6), 759–768 (2010).
10. T. Y. Ohulchanskyy, I. Roy, K. T. Yong, H. E. Pudavar, and P. N. Prasad, "High-resolution light microscopy using luminescent nanoparticles," Wiley Interdiscip Rev Nanomed Nanobiotechnol **2**(2), 162–175 (2010).
11. D. J. Bharali, I. Klejbor, E. K. Stachowiak, P. Dutta, I. Roy, N. Kaur, E. J. Bergey, P. N. Prasad, and M. K. Stachowiak, "Organically modified silica nanoparticles: a nonviral vector for in vivo gene delivery and expression in the brain," Proc. Natl. Acad. Sci. U.S.A. **102**(32), 11539–11544 (2005).

#130218 - $15.00 USD Received 15 Jun 2010; revised 24 Jul 2010; accepted 26 Jul 2010; published 2 Aug 2010

12. T. Y. Ohulchanskyy, I. Roy, L. N. Goswami, Y. H. Chen, E. J. Bergey, R. K. Pandey, A. R. Oseroff, and P. N. Prasad, "Organically modified silica nanoparticles with covalently incorporated photosensitizer for photodynamic therapy of cancer," Nano Lett. **7**(9), 2835–2842 (2007).
13. S. Kim, T. Y. Ohulchanskyy, H. E. Pudavar, R. K. Pandey, and P. N. Prasad, "Organically modified silica nanoparticles co-encapsulating photosensitizing drug and aggregation-enhanced two-photon absorbing fluorescent dye aggregates for two-photon photodynamic therapy," J. Am. Chem. Soc. **129**(9), 2669–2675 (2007).
14. J. Qian, X. Li, M. Wei, X. Gao, Z. Xu, and S. He, "Bio-molecule-conjugated fluorescent organically modified silica nanoparticles as optical probes for cancer cell imaging," Opt. Express **16**(24), 19568–19578 (2008).
15. R. Kumar, I. Roy, T. Y. Ohulchanskyy, L. N. Goswami, A. C. Bonoiu, E. J. Bergey, K. M. Tramposch, A. Maitra, and P. N. Prasad, "Covalently dye-linked, surface-controlled, and bioconjugated organically modified silica nanoparticles as targeted probes for optical imaging," ACS Nano **2**(3), 449–456 (2008).
16. I. Brigger, C. Dubernet, and P. Couvreur, "Nanoparticles in cancer therapy and diagnosis," Adv. Drug Deliv. Rev. **54**(5), 631–651 (2002).
17. A. C. Antony, "Folate receptors," Annu. Rev. Nutr. **16**(1), 501–521 (1996).
18. C. P. Leamon, and J. A. Reddy, "Folate-targeted chemotherapy," Adv. Drug Deliv. Rev. **56**(8), 1127–1141 (2004).
19. Y. Lu, and P. S. Low, "Folate-mediated delivery of macromolecular anticancer therapeutic agents," Adv. Drug Deliv. Rev. **54**(5), 675–693 (2002).
20. C. Sun, R. Sze, and M. Zhang, "Folic acid-PEG conjugated superparamagnetic nanoparticles for targeted cellular uptake and detection by MRI," J. Biomed. Mater. Res. A **78**(3), 550–557 (2006).
21. J. H. Park, L. Gu, G. von Maltzahn, E. Ruoslahti, S. N. Bhatia, and M. J. Sailor, "Biodegradable luminescent porous silicon nanoparticles for in vivo applications," Nat. Mater. **8**(4), 331–336 (2009).
22. S. Yao, H. Y. Ahn, X. Wang, J. Fu, E. W. Van Stryland, D. J. Hagan, and K. D. Belfield, "Donor-acceptor-donor fluorene derivatives for two-photon fluorescence lysosomal imaging," J. Org. Chem. **75**(12), 3965–3974 (2010).
23. J. R. Lakowicz, *Principles of Fluorescence Spectroscopy*, (Kluwer Academic / Plenum Publisher, New York, Second Edition, 52–53, 1999).
24. C. C. Corredor, K. D. Belfield, M. V. Bondar, O. V. Przhonska, and S. Yao, "One- and two-photon photochemical stability of linear and branched fluorene derivatives," J. Photochem. Photobiol. Chem. **184**(1-2), 105–112 (2006).
25. K. D. Belfield, M. V. Bondar, C. O. Yanez, F. E. Hernandez, and O. V. Przhonska, "One- and two-photon stimulated emission depletion of a sulfonyl-containing fluorene derivative," J. Phys. Chem. B **113**(20), 7101–7106 (2009).
26. H. Shi, X. He, Y. Yuan, K. Wang, and D. Liu, "Nanoparticle-based biocompatible and long-life marker for lysosome labeling and tracking," Anal. Chem. **82**(6), 2213–2220 (2010).
27. E. I. Sega, and P. S. Low, "Tumor detection using folate receptor-targeted imaging agents," Cancer Metastasis Rev. **27**(4), 655–664 (2008).

1. Introduction

Two-photon fluorescence microscopy (2PFM) has several advantages in biological imaging over conventional one-photon fluorescence microscopy (1PFM), including high three-dimensional (3D) spatial localization due to the inherent nonlinear dependence of two-photon fluorescence (2PF) on the illumination intensity [1,2], deeper penetration into optically thick tissue, and improved tissue viability because of using near-IR excitation [3,4]. We have reported a number of fluorene-based molecules that undergo good two-photon absorption (2PA). However, 2PA fluorenyl fluorophores with high fluorescence quantum efficiency are synthetically more accessible in hydrophobic forms [5–7]. The incompatibility to aqueous biological systems limits their application in biological imaging area. Our efforts are directed to overcome these limitations as described herein.

Nanomaterials are beginning to revolutionize the fields of medicine, bioimaging, and photonics due to their chemical and biological resilience, safety, and multimodality of the surface [8–10]. In the past few years, ceramic-based nanomaterials have proven to be innocuous and have been widely investigated in the application of gene delivery as DNA carriers [11], photodynamic therapy as carriers of photosensitizers [12,13], and bioimaging as nanoprobes [14,15]. In this paper, organically modified silica (ORMOSIL) nanoparticles were employed to encapsulate hydrophobic fluorenyl dyes to provide a stable aqueous dispersion of the fluorescent probe and improve the fluorophore's photostability. Narrow dispersity ORMOSIL nanoparticles (diameter ~25 nm), entrapping a hydrophobic two-photon absorbing fluorenyl dye 4,4'-(1E,1'E)-2,2'-(9,9-didecyl-9H-fluorene-2,7-diyl)bis(ethene-2,1-

#130218 - $15.00 USD Received 15 Jun 2010; revised 24 Jul 2010; accepted 26 Jul 2010; published 2 Aug 2010

diyl)bis(N,N-dibutylaniline) (DBF), were synthesized in the nonpolar core of Aerosol-OT micelles by hydrolysis of triethoxyvinylsilane and (3-aminopropyl)triethoxysilane. To introduce targeting specificity, the surface of the SiNPs was further functionalized by a cell receptor targeted ligand.

With the development of cell biology, a variety of disease-specific ligand-receptor pairs have been identified, e.g., ligands based on antibodies, antibody fragments, proteins, and peptides. Because of their high selectivity towards specific cell receptors, those biomolecules were conjugated to nanoparticles and investigated for specific targeting delivery [16]. One example of such a ligand-receptor pair is folate ligand and folate receptor (FR). FR is found over-expressed in a number of human cancer cell while the distribution in normal tissues is minimal. The folate ligand, which is a member of vitamin B family, plays an important role in cell survival by its participation in the biosynthesis of nucleic and amino acids [17]. It is also a high affinity ligand that enhances conjugated anti-cancer drugs by targeting folate receptor (FR) positive cancer cells [18]. In this work, a most commonly used folate ligand, folic acid, was introduced on the surface of dye-doped SiNPs, not only because it can efficiently internalize into the cell through receptor mediated endocytosis when conjugated with a variety of biomolecules, but, significantly, folic acid is stable and low cost [19].

The nanoparticle probes were structurally characterized while spectroscopic analyses demonstrated that the optical properties of the incorporated dye were retained. Moreover the photostability of the dye improved significantly by encapsulation within the SiNPs. *In vitro* studies using Hela cells that overexpress FRs revealed cellular uptake of the folate nanoparticles. Meanwhile MG63 cells, which do not express FR, did not uptake the folate SiNPs efficiently [20]. Furthermore, Hela cells, whose FRs were first blocked by free folic acid, were incubated with the folic acid conjugated SiNPs, resulting in a dramatic decrease in the uptake of the folic acid conjugated SiNPs. These finding demonstrated that the folic acid functionalized SiNPs have *in vitro* cell specificity, while mainting good 2PA, fluorescence, and photostability properties, making these 2PA modified SiNPs useful tools as for two-photon optical bioimaging [21].

2. Experimental

2.1. Materials

Triethoxyvinylsilane (VTES, 97%), cosurfactant 1-butanol (99%), surfactant Aerosol OT (AOT, 98%). Dioctylsulfosuccinate sodium salt and (3-aminopropyl)triethoxysilane (APTES) were purchased from Sigma-Aldrich. N-methyl-2-pyrrolidinone (NMP, 99%) was purchased from Acros Organic. Thermo Slide-A-Lyzer® 10K cut off dialysis cassettes and 0.22 μm cutoff membrane filter were purchased from Fisher Inc. All the above chemicals were used as received without further purification unless noted. Hela and MG63 cells were purchased from ATCC (America Type Culture Collection, Manssas, VA). All cells were incubated in RPMI-1640 medium (Invitrogen, Carlsbad, CA), supplemented with 10% fetal bovine serum (FBS, Atlanta Biologicals, Lawrenceville, GA), 100 units/mL penicillin-streptomycin (Atlanta Biologicals, Lawrenceville, GA), and incubated at 37 °C in a 95% humidified atmosphere containing 5% CO_2. Details of fluorenyl derivative DBF, including preparation and characterization, were described in ref. 22 [22].

2.2. Synthesis of dye-encapsulated amine-terminated silica nanoparticles

Amine-terminated SiNPs, with or without fluorenyl derivative DBF, were synthesized according to the method described by P. N. Prasad et al. [15]. The synthesis of silica nanoparticles and their bioconjugation with folic acid was schematically described by Fig. 1. Briefly, the nanoparticles were synthesized in the nonpolar core of AOT/1-butanol micelles in deionized water. NMP was used as a hydrophilic solvent which has unlimited water miscibility as well as suitable solubility for DBF. First, 0.22 g of the surfactant AOT, 300 μL

#130218 - $15.00 USD Received 15 Jun 2010; revised 24 Jul 2010; accepted 26 Jul 2010; published 2 Aug 2010

of the cosurfactant 1- butanol, and 100 μL of NMP were dissolved in 10 mL deionized water with magnetic stirring, forming an oil-in-water microemulsion. To the microemulsion system, 100 μL of neat NMP or NMP solutions containing DBF dye (2 mg / mL) was added, followed by addition 100 μL of neat VTES. After stirring the reaction mixture for one additional hour, the polymerization reaction was initialized by the addition of 20 μL neat APTES. To ensure completion of polymerization within the coprecipitated nanoparticles, the mixtures were further stirred at room temperature for 20 h. Nanoparticle purification was conducted by dialysis against deionized water in a 10 kDa cutoff cellulose membrane to remove surfactant, cosurfactant, and other unreacted molecules for 48 h. The dialyzed solution was then filtered through a 0.22 μm cutoff membrane filter and stored at 5 °C for later use.

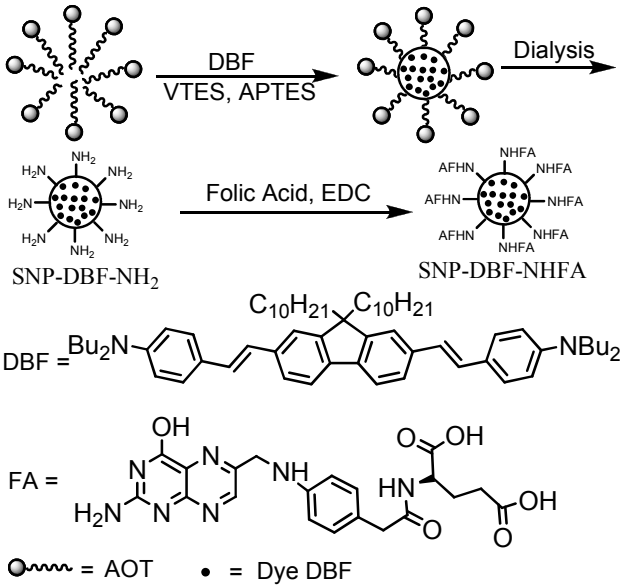

Fig. 1. Schematic illustration of the synthesis of silica nanoparticles and their bioconjugation with folic acid.

2.3. Conjugation of amine-terminated silica nanoparticles with folic acid

To a 5 mL portion of stock solution of amine-terminated DBF dye-doped or unlabeled nanoparticles, 200 μL of 0.1 M EDC solution was added, and the mixture was stirred at r. t. for 30 min. Then, an excess of folic acid (2 mg) was added, and the reaction between folic acid and amino groups was allowed to proceed for 3 h. The reaction mixture was dialyzed against deionized water for 50 h to remove unreacted molecules. Finally, all the samples were filtered through a 0.22 μm cutoff membrane filter and stored at 5 °C for later use.

2.4. Characterization of dye-encapsulated silica nanoparticles

Transmission electron microscopy (TEM) images were obtained using a JEOL-JEM 1011 Transmission electron microscope (Manufacturer: JEOL, Ltd., Japan.) operating at 100 kV n bright field for the SiNPs. A drop of nanoparticles dispersed in water was placed on a holey carbon film copper grid and left to evaporate. The bioconjugation of the SiNPs with folic acid was confirmed by comparing the optical spectra of the SiNPs.

2.5. Linear photophysical characterization

Linear photophysical properties of DBF and the SiNPs, including absorption, fluorescence, excitation, anisotropy, and fluorescence lifetime, were investigated in spectroscopic grade THF or ultrapure deionized water at room temperature. The steady-state absorption spectra

#130218 - $15.00 USD Received 15 Jun 2010; revised 24 Jul 2010; accepted 26 Jul 2010; published 2 Aug 2010

were measured with an Agilent 8453 UV-visible spectrophotometer in 10 mm path length quartz cuvettes. The steady-state fluorescence, excitation, and fluorescence anisotropy spectra were measured with PTI QuantaMaster spectrofluorimeter in 10 mm spectrofluorometric quartz cuvettes, with dye concentrations ~(1–1.5) × 10^{-6} M. Fluorescence lifetimes of the free dye and nanoparticles were measured with a single photon counting system PicoHarp 300 under 76 MHz femtosecond excitation (MIRA 900, Coherent) with time resolution of ≈80 ps. The values of fluorescence quantum yield of DBF in THF and SiNPs in water were determined relative to 9, 10-diphenylanthracene in cyclohexane (Φ = 0.90) as a standard [23]. All optical densities of the dye DBF, silica nanoparticles, and standard were less than 0.1.

2.6. Photostability measurement

The photostabilities of DBF in THF and SiNPs suspended in water were measured by irradiation of solutions of DBF in THF or SiNPs in water in 1 mm path length quartz cuvettes using a 405 nm diode laser at 20 mW [24]. Irradiation time-dependent absorption spectra were obtained with an Agilent 8453 UV/Vis spectrophotometer with an initial OD of ~1.5. For comparison, the photostability of fluorescein was measured by irradiation of solutions of fluorescein in 0.1 M NaOH(aq) in 1 mm path length quartz cuvettes by a 501 nm argon ion laser at 2.1 mW. Absorption spectra were recorded with an initial OD of ~1.6. Photodecomposition quantum yields, Φ, were calculated according to Eq. (1), and the result shown in Table 1 is the average of ten pairs of adjacent maximum absorption values.

$$\Phi = \frac{(A_1 - A_0)N_A}{10^3 \times \varepsilon \times \mathrm{I} \times (1 - 10^{(A_1 + A_0)/2})(t_1 - t_0)} \quad (1)$$

where Φ is the photodecomposition quantum yield, A_1 is absorbance maximum at t_1, A_0 is absorbance maximum at t_0, N_A is Avogadro's number, ε is molar absorbance, t_1-t_0 is exposure time (s), and I is the intensity in photon · sec^{-1} · cm^{-2}.

2.7. Determination of two-photon cross section

The 2PA spectrum of DBF was determined over a broad spectral region by the typical two-photon induced fluorescence (2PF) method relative to Rhodamine B in methanol as a standard [25]. A PTI QuantaMaster spectrofluorimeter and femtosecond Ti: sapphire laser (Mira 900F, 220 fs pulse width, 74 MHz repetition rate, Coherent, USA), tuning range 700–940 nm, were used. Two-photon fluorescence measurements were performed in 10 mm fluorometric quartz cuvettes with dye concentrations ~1.5 × 10^{-5} M in THF. The experimental fluorescence excitation and detection conditions were conducted with negligible reabsorption. The quadratic dependence of two-photon induced fluorescence intensity on the excitation power was verified for each excitation wavelength.

2.8. Cytotoxicity Assay

To test the cytotoxicity of the folate-modified SiNPs, 4 × 10^3 per well of Hela cells or MG63 cells in 96-well plates were incubated for 24 h in 90 μL of RPMI-160 medium without phenol red, supplemented with 10% FBS and 100 units / mL penicillin-streptomycin. Then cells were then incubated with various amounts of silica nanoparticles SNP-DBF-NHFA (30 μM, 20 μM, 10 μM, 5 μM, 1 μM) for an additional 20 h. Subsequently, 20 μL of CellTiter 96® AQueous One Solution reagent was added into each well, followed by incubation for an additional 4 h at 37 °C. The relative viability of the cells incubated with the SiNPs relative to untreated cells was determined by measuring the MTS-formazan absorbance on a Kinetic microplate reader (Spectra Max M5, Molecular Devices, Sunnyvale, CA, USA) at 490 nm with a subtraction of the absorbance of cell-free blank volume at 490 nm. The results from three individual experiments were averaged.

#130218 - $15.00 USD Received 15 Jun 2010; revised 24 Jul 2010; accepted 26 Jul 2010; published 2 Aug 2010

2.9. Uptake of silica nanoparticles in cancer cells

Hela cells or MG63 cells were placed onto poly-D-lysine coated glasses in 24-well plates (40,000 cells per well), and the cells were incubated for 48 h before incubating with dye-doped SiNPs. A stock solution of dye-doped SiNPs suspended in water was prepared as 0.5 mM solution. The solution was diluted to a 10 μM, 20 μM, and 50 μM by complete growth medium, RPMI-1640, and then freshly placed over the cells for a 2 h period. After incubation, cells were washed with PBS (3–5X) and fixed using 3.7% formaldehyde solution for 15 min at 37 °C. To reduce autofluorescence, a fresh solution of $NaBH_4$ (1 mg/mL) in PBS (pH = 8.0), which was prepared by adding few drops of 6N NaOH solution into PBS (pH = 7.2), was used for treating the fixed cells for 15 min (2X). The plates were then washed twice with PBS and finally water. Subsequently, glass covers were mounted with Prolong gold mounting medium for microscopy.

2.10. 1PFM, 2PFM and two-photon FLIM imaging

Conventional single-photon fluorescence images were obtained using an inverted microscope (Olympus IX70) equipped with a QImaging cooled CCD (Model Retiga EXi) and excitation with a 100 W mercury lamp. In order to improve the fluorescence background-to-image ratios, one-photon confocal fluorescence images of the fixed cells were obtained using a custom made filter cube (Ex: 377/50; DM: 409; Em:525/40) for the dye-doped SiNPs. The specifications of the filter cube were tailored to match the excitation wavelength of probes and to capture most of its emission profile. 2PFM and 2P-FLIM imaging were performed by a modified Olympus Fluoview FV300 microscope system coupled to a tunable Coherent Mira 900F Ti:sapphire (76 MHz, modelocked, femtosecond laser tuned to 740 nm), and a compact FLIM system from PicoQuant. An emission short-pass filter (cutoff 690 nm) was placed in the microscope scanhead to avoid background irradiance from the excitation source. Consecutive layers, separated by approximately 0.15 μm, were recorded to create a 3D reconstruction from overlaid 2PFM images. The two-photon induced fluorescence was collected with a 60 × microscope objective (UPLANSAPO 60x, NA = 1.35, Olympus). For 2P-FLIM imaging, the output fluorescence was delivered to an avalanche photodiode (APD) detector (PicoQuant, Germany). A band-pass filter (500nm −700 nm) was placed in front of the APD detector. Data were acquired using theTime Harp 300 module and software package *SymPhoTime* (PicoQuant, Germany).

3. Results and discussion

The morphology and size of the DBF-doped SiNPs were determined by TEM images (Fig. 2). The particle size distribution determined by the TEM images indicated that they were of narrow dispersity, with a diameter range of 25-40 nm. The average particle size of the dye-doped amino-terminated silica nanoparticles (SNP-DBF-NH_2) was 30 nm. After the particles were conjugated with folic acid, their average particle size increased to 34 nm. The increase in particle size is apparently attributed to the shielding of their surface by folic acid. In addition, the absorbance of 272 nm in the folic acid functionalized nonlabeled silica nanoparticles (SNP-NHFA) and folate dye-doped silica nanoparticles (SNP-DBF-NHFA) also indicated successful conjugation of the folic acid with the silica nanoparticles (Fig. 3a). Moreover, the presence of the folic acid on the surface of the SiNPs was demonstrated by comparing the anisotropy, excitation, and emission spectra of the nonlabeled amino-terminated silica nanoparticles (SNP-NH_2) and SNP-NHFA in water. The concentration of dye in SNP-DBF-NHFA was determined by absorbance at 410 nm ($\varepsilon_{410\ nm} = 7.1 \times 10^4\ M^{-1}cm^{-1}$ in water). The final concentration of SNP-DBF-NHFA in water was 2.3 mg/mL, determined by vaporization.

#130218 - $15.00 USD Received 15 Jun 2010; revised 24 Jul 2010; accepted 26 Jul 2010; published 2 Aug 2010

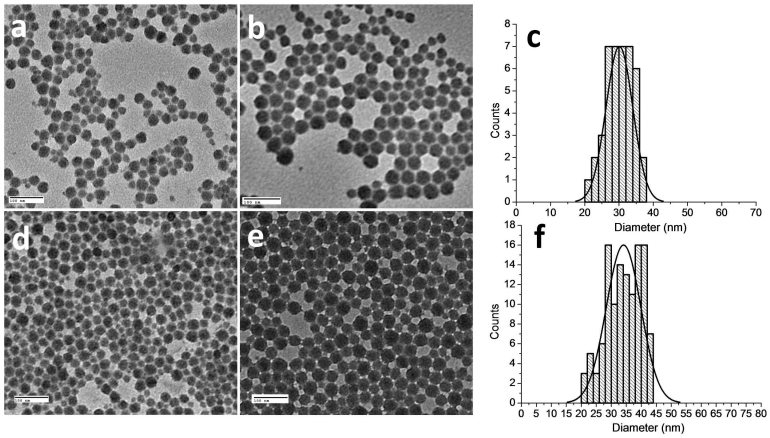

Fig. 2. TEM images of silica nanoparticles (a) SNP-NH_2, (b) SNP-DBF-NH_2, and (c) their particle size distribution, (d) SNP-NHFA, (e) SNP-DBF-NHFA, and (f) their particle size distribution. Scale bar: 100 nm.

The linear and nonlinear photophysical properties of the SiNPs were investigated to assess their potential for two-photon bioimaging. The absorption, excitation, and fluorescence spectra of the SiNPs suspended in water, as well as the free DBF dye in THF, are shown in Fig. 3. The spectra of dye-doped SiNPs were similar to the spectra of the free DBF in THF, except for the expected absorbance of folic acid at 272 nm in the folate SiNPs. The spectra of unlabeled folate silica nanoparticles (SNP-NHFA) exhibited absorbance and excitation of folic acid at 272 and 360 nm, and very weak fluorescence of the folic acid with maximum emission at 476 nm, which was not present in the spectra of folic acid-free unlabeled silica nanoparticles (SNP-NH_2).

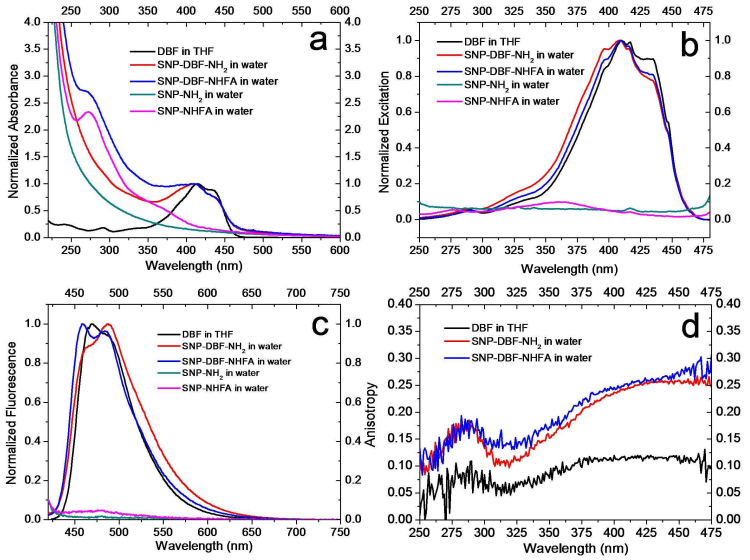

Fig. 3. (a) Normalized absorption of DBF in THF and SiNPs in water, (b) normalized excitation spectra of DBF in THF and SiNPs in water, the maximum excitation of SNP-NH_2 and SNP-NHFA were normalized to 0.1 (Em: 490 nm), (c) normalized fluorescence emission spectra of DBF in THF and SiNPs in water, the maximum fluorescence of SNP-NH_2 and SNP-NHFA were normalized to 0.1 (Ex: 410 nm), and (d) fluorescence anisotropy of DBF in THF and SiNPs in water (Em: 490 nm).

#130218 - $15.00 USD Received 15 Jun 2010; revised 24 Jul 2010; accepted 26 Jul 2010; published 2 Aug 2010

The fluorescence anisotropy of SNP-DBF-NH2, SNP-DBF-NHFA suspended in water and the free dye in THF (Fig. 3d) indicates that the fluorescence of the dye doped in the particles manifests relative high anisotropy, just as in very viscous solvent pTHF [15] while the free dye in THF exhibited much lower fluorescence anisotropy. This result can be explained by the fact that the rotational mobility of the dye molecules within the SiNPs was limited. Although the fluorescence quantum yield, φ, of the dye in SiNPs suspended in water decreased to 0.49 from 1.0 in organic solvent, due to likely aggregation, its photostability improved nearly 7 times when it was encapsulated in the SiNPs. The photostability of the dye-doped SiNPs nanoparticles and free dye in THF were compared with the common fluorescent dye fluorescein. The photobleaching decomposition quantum yield of fluorescein was 7.3×10^{-6}, approximately 4 times higher than DBF in THF and 28 times higher than SNP-DBF-NHFA in water. The photostability results and the photophysical properties of SNP-DBF-NHFA suspended in water and the free dye in THF are summarized and compared with fluorescein in Table 1. The florescence decays of the free dye in THF and SNP-DBF-NHFA suspended in water were characterized by a single exponential process. The fluorescence life time, $\tau \approx 1.2$ ns, of DBF remained almost the same after encapsulation in SiNPs. The efficiency 2PA for free DBF in relatively high polarity solution, THF, which is close to water, was investigated. The 2PA cross sections were determined in the range of 700-940 nm, a useful range for 2PFM, and are presented in Fig. 4a. The dye showed a maximum 2PA cross section value of ~400 GM at 740 nm, which is quite suitable for 2PFM bioimaging using commercially available femtosecond lasers.

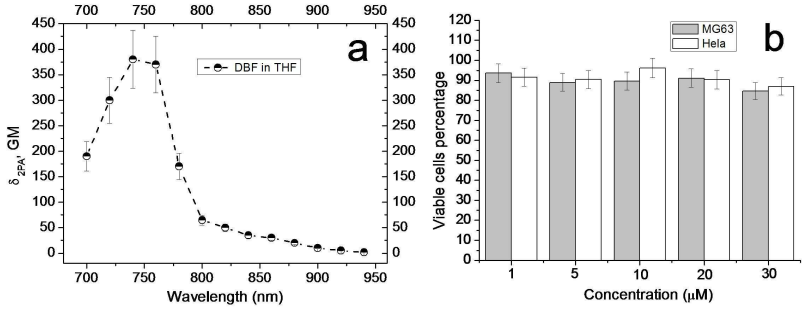

Fig. 4. (a) 2PA cross sections of DBF (fs excitation). (b) Viability of Hela and MG63 cells with SNP-DBF-NHFA.

Table 1. Photophysical properties of the DBF in THF, SNP-DBF-NHFA in water and fluorescein in 0.1 M NaOH aqueous solution

Materials	$\lambda_{max}^{(ex)} / \lambda_{max}^{(fl)}$ [a]	$\varepsilon \cdot 10^{-4}$ [b]	τ [c]	φ [d]	$\Phi \cdot 10^{6}$ [e]
DBF	410/470	10.1	1.25 ± 0.08	1.0	1.9
SNP-DBF-NHFA	409/458	7.1	1.20 ± 0.08	0.49	0.26
Fluorescein	491/521	8.8	n.d.[f]	0.95	7.3

[a] λ_{max} values of the one-photon excitation and emission spectra in nm; [b] molar absorbance in $M^{-1} \cdot cm^{-1}$; [c] fluorescence lifetime in ns; [d] fluorescence quantum yield, ± 15%; [e] photodecomposition quantum yield, ± 15%; [f] Not determined.

Cytotoxicity of the SiNPs must be minimized if the particles are to be used as probes for 2PFM imaging in living cells. An MTS viability test with Hela and MG63 cells was performed to determine the cytotoxicity of the folate dye-doped SiNPs The results presented in Fig. 4b indicates that the toxicity of the nanoparticles is very low (~90% viability) over a concentration range from 1 – 30 μM, after treating the Hela and MG63 cells with a variety of concentrations of nanoparticles for 24 h. The concentrations were determined by the absorbance of the SiNPs at 410 nm.

#130218 - $15.00 USD Received 15 Jun 2010; revised 24 Jul 2010; accepted 26 Jul 2010; published 2 Aug 2010

To test the selectivity of the folate dye-doped SiNPs *in vitro*, Hela cells, known to overexpress FRs, were employed as a positive control while low folate receptor expressing cancer cells MG63 were selected as a negative control [17]. One-photon and two-photon fluorescence microscopy was used to study the selective uptake of the folate silica nanoparticles SNP-DBF-NHFA between Hela and MG63 cells. The fluorescence images of Hela and MG63 cells incubated with folate silica nanoparticles SNP-DBF-NHFA, shown in Fig. 5, indicated that SNP-DBF-NHFA was specifically taken by FR overexpressing Hela cells. However, the low FR expressing MG63 cells (Fig. 5 middle row) did not take the folate nanoparticles effectively. To confirm that the uptake of the folate nanoparticles by Hela cells is mediated by the FR, Hela cells whose FR were initially blocked by free folic acid were used to incubate with SNP-DBF-NHFA. The result (bottom row of Fig. 5) indicated that the Hela cells did not uptake the folate silica nanoparticles to any large degree after their FRs were blocked by folic acid. This enhanced efficiency is attributed to receptor-mediated uptake of these folate nanoparticles with the FR of Hela cells.

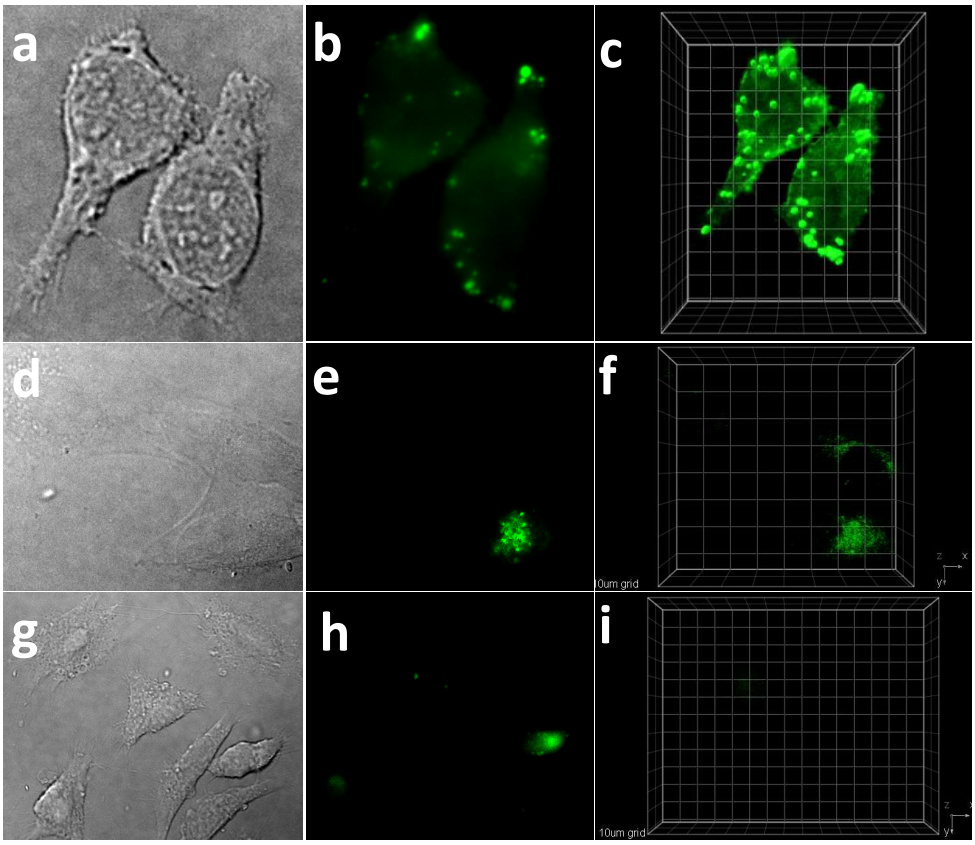

Fig. 5. Images of Hela cells (top row), MG63 cells (middle row), and folate receptor blocked Hela cells (bottom row) incubated with SNP-DBF-NHFA (20 μM, 2 h). Left column: DIC, 40 ms. Middle column: one-photon fluorescence image, 200 ms (filter cube Ex: 377/50 DM: 409 Em: 525/40). Right column: 3D reconstruction from overlaid two-photon fluorescence images (Ex: 740 nm; Power: 30 mW; Em. short-pass filter 690 nm) 10 μm grid.

Moreover, 2PFM and 2P-FLIM images (Fig. 6) of Hela cells incubated with SNP-DBF-NHFA were performed to show the distribution of nanoparticles in the cells. The resulting 2PFM and 2P-FLIM images clearly illustrate organelles in the cytoplasm of cells. The organelles are spherical in shape with an average diameter of ~600 nm, likely lysosomes or endosomes in term of their size and morphology [26]. The average fluorescence lifetime of

#130218 - $15.00 USD Received 15 Jun 2010; revised 24 Jul 2010; accepted 26 Jul 2010; published 2 Aug 2010

the SiNP probe within the organelles was ~1.2 ns, consistent with that observed for the dye-doped SiNPs in water, further confirming successful SNP-DBF-NHFA up take by Hela cells.

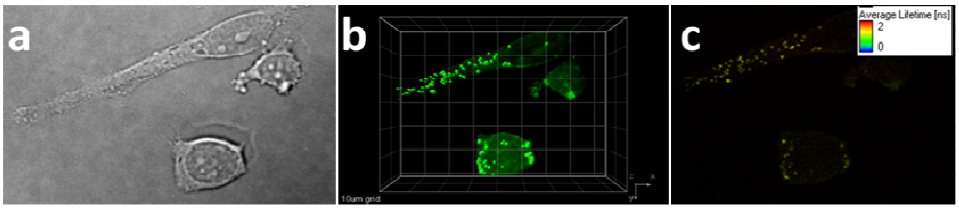

Fig. 6. Images of Hela cells incubated with SNP-DBF-NHFA (20 μM, 2 h). (a) DIC, 20 ms, (b) 3D reconstruction from overlaid two-photon fluorescence images (Ex: 740 nm; Power: 30 mW; Em. short-pass filter 690 nm) 10 μm grid, (c) 2P-FLIM image (Ex: 740 nm; Power: 30 mW).

4. Conclusion

Narrow dispersity organically-modified SiNPs, entrapping a hydrophobic 2PA fluorescent dye, were synthesized and characterized. In order to specifically deliver the two-photon fluorescent SiNPs to cancer cells, the surface of the nanoparticles were functionalized with folic acid. Significantly, the photostability of the fluorescent silica nanoparticles was seven times greater than the free dye and 28 times greater than the commercially available dye fluorescein. Cytotoxicity of the folate-modified dye-containing SiNPs was low. The folate-modified dye-containing SiNPs were selectively taken by folate receptor overexpressing Hela cells, as determined by 1PFM, 2PFM, and 2P-FLIM imaging experiments. Thus, these folate-modified dye-containing SiNPs are excellent candidates as efficient probes for 2PFM and 2P-FLIM bioimaging applications, and have prospective application for earlier diagnosis of folate receptor overexpressed cancers, including breast, ovary, endometrium, and lungs cancer [27].

Acknowledgments

We wish to acknowledge the National Institutes of Health (1 R15 EB008858-01), the U.S. Civilian Research and Development Foundation (UKB2-2923-KV-07), the Ministry of Education and Science of Ukraine (grant M/49-2008), and the National Science Foundation (CHE-0832622 and CHE-0840431) for support of this work.

#130218 - $15.00 USD Received 15 Jun 2010; revised 24 Jul 2010; accepted 26 Jul 2010; published 2 Aug 2010